Neurospine 2022;19(3):501-512.
https://doi.org/10.14245/ns.2244222.111

Neurospine
pISSN 2586-6583 eISSN 2586-6591

Original Article

Safety and Feasibility of Augmented Reality Assistance in Minimally Invasive and Open Resection of Benign Intradural Extramedullary Tumors

Corresponding Author
Roger Härtl
https://orcid.org/0000-0003-2442-8944

Department of Neurosurgery, New York-Presbyterian Hospital, 525 E 68th Street, Box 99, New York, New York 10065, USA
Email: roh9005@med.cornell.edu

Received: March 9, 2022
Revised: April 26, 2022
Accepted: April 27, 2022

Fabian Sommer, Ibrahim Hussain, Sertac Kirnaz, Jacob Goldberg, Lynn McGrath, Rodrigo Navarro-Ramirez, Francois Waterkeyn, Franziska Schmidt, Pravesh Shankar Gadjradj, Roger Härtl

Department of Neurosurgery, Weill Cornell Medicine, New York Presbyterian Hospital/Och Spine, New York, NY, USA

Objective: Surgical resection of benign intradural extramedullary tumors (BIETs) is effective for appropriately selected patients. Minimally invasive surgical (MIS) techniques have been described for successful resection of BIET while minimizing soft tissue injury. Augmented reality (AR) is a promising new technology that can accurately allow for intraoperative localization from skin through the intradural compartment. We present a case series evaluating the timing, steps, and accuracy at which this technology is able to enhance BIET resection.
Methods: A protocol for MIS and open AR-guided BIET resection was developed and applied to determine the feasibility. The tumor is marked on diagnostic magnetic resonance imaging (MRI) using AR software. Intraoperatively, the planning MRI is fused with the intraoperative computed tomography. The position and size of the tumor is projected into the surgical microscope and directly into the surgeon's field of view. Intraoperative orientation is performed exclusively via navigation and AR projection. Demographic and perioperative factors were collected.
Results: Eight patients were enrolled. The average operative time for MIS cases was 128 ± 8 minutes and for open cases 206 ± 55 minutes. The estimated intraoperative blood loss was 97 ± 77 mL in MIS and 240 ± 206 mL in open procedures. AR tumor location and margins were considered sufficiently precise by the surgeon in every case. Neither correction of the approach trajectory nor ultrasound assistance to localize the tumor were necessary in any case. No intraoperative complications were observed.
Conclusion: Current findings suggest that AR may be a feasible technique for tumor localization in the MIS and open resection of benign spinal extramedullary tumors.

Keywords: Minimally invasive surgery, Benign extramedullary intradural tumor, Augmented Reality, benign intradural extramedullary tumor

INTRODUCTION

Benign spinal extramedullary tumors (BIETs) are a complex clinical entity affecting patients of all ages.[1] Due to narrowing space in the intradural compartment, these tumors often cause pain and neurological symptoms related to compression of the neural elements.[2]

Surgical excision is indicated for BIETs with progressive clinical symptoms, radiographic growth, and decreased quality of life.[2,3] Where possible, the tumor should be entirely resected while simultaneously preserving neural integrity and as much surrounding tissue as possible.[2,3] Localization of the surgical

level(s) is typically performed by confirming the level of pathology from the preoperative magnetic resonance imaging (MRI) with intraoperative x-rays. The transfer of the tumor location from MRI images to the patient's radiographic anatomy for localization is the obligation of the surgeon. Surgical approaches often require more soft tissue and muscle dissection than necessary, especially in obese patients, resulting in higher approach-specific morbidity. Following laminectomy, intradural tumor location can be confirmed via sonography to determine the extent of dural opening.[4] Until recently, this was a prohibitive criterion for minimally invasive approaches, as traditional "hockey-stick" ultrasound transducer probes could not fit through the tubular retractor.[5,6] Nonetheless, evolutions in technology were sought so that patients undergoing BIET resection could benefit from the established advantages of tubular minimally invasive surgical (MIS) procedures, including lower blood loss, infection risk, less postoperative pain/opioid usage, shorter hospital length of stay, and preservation of the posterior tension band.[5]

Augmented reality (AR) is an emerging technology that allows the surgeon to highlight anatomically relevant key structures and pathologies, which are displayed in the microscope's field of view during surgery.[7] For spinal tumor surgery, this technology can be particularly helpful since it can support the surgeon from the beginning of the surgery during incision planning and tubular insertion trajectory, thus minimizing soft tissue injury. Once the bony anatomy is exposed, highlighting of the tumor precisely determines how much bony resection is required for adequate dural exposure. Additionally, AR can localize the tumor in the crani-caudal as well as mediolateral dimensions, which is especially helpful for laterally positioned tumors that require medial facetectomy, since this can help minimize iatrogenic instability. These advantages could be particularly helpful when using surgical approaches with limited visualization for resection of BIETs, as with tubular MIS approaches.

The use of an early version of AR for the open resection of cervical and thoracic intradural tumors has been described with promising results from Carl et al.[8] We have developed a protocol for how to implement AR for the resection of BIET and evaluated the clinical feasibility of this technique in a case series of open and tubular minimally invasive approaches. To our knowledge, this is the first description of AR-assisted resection of BIET via the tubular minimally invasive approach as well as the use of AR for lumbar tumors.

MATERIALS AND METHODS

1. Patient Characteristics

We conducted a prospective case study of AR-assisted resection of BIET between 11/20 and 08/21 at a single tertiary medical center.

Age, sex, American Society of Anesthesiologists (ASA) physical status classification, body mass index (BMI), and neurological symptoms were collected. In addition, intraoperative blood loss, complications, and the length of hospital stay were recorded. Clinical evaluation including sensorimotor examination and wound assessment was performed immediately postoperatively and 2 weeks after surgery.

2. AR Application

The AR application was planned utilizing Brainlab (Munich, Germany) Element's software. Planning was based on the MRI images available as part of the diagnostic workup of the patient's pathology. The MRI should have a high resolution with slices not exceeding 2 mm in thickness to avoid inaccuracy. The tumor was highlighted using the software's "smart brush" function, which uses automatic algorithms to merge the structures highlighted on individual plane (2-dimensional, 2D) layers into a structured (3-dimensional, 3D) shape. Additionally, the software was used to calculate the tumor volume based on the highlighting on the MRI. The software fused the 2D markings to a 3D model of the tumor. This allowed even the calculation of irregular shaped tumors (Fig. 1).

The decision if a MIS or open tumor resection was performed was based on the suspected tumor pathology, size, and the location. Based on our experience, the MIS tubular approach is most suitable for small, benign tumors located in the lumbar spine.

To facilitate the surgeon's orientation to the surgical site, the closest disc space was also highlighted and, if desired, projected into the microscope's view. The surgeries were performed using total 3D navigation and the setup of the operating room was the same as a standard navigated surgery with navigation system and infrared cameras.[9] The only additional equipment was a navigation array that was attached to the microscope to enable tracking by the navigation system (Fig. 2).

At the beginning of each procedure, an intraoperative low-dose navigation computed tomography (CT) was performed. Subsequently, the preoperative MRI, including the highlighted structures, was fused with the intraoperative navigation CT to transfer the localization of the tumor from the MRI to the CT image. Since the intraoperative CT was performed in prone po-

https://doi.org/10.14245/ns.2244222.111

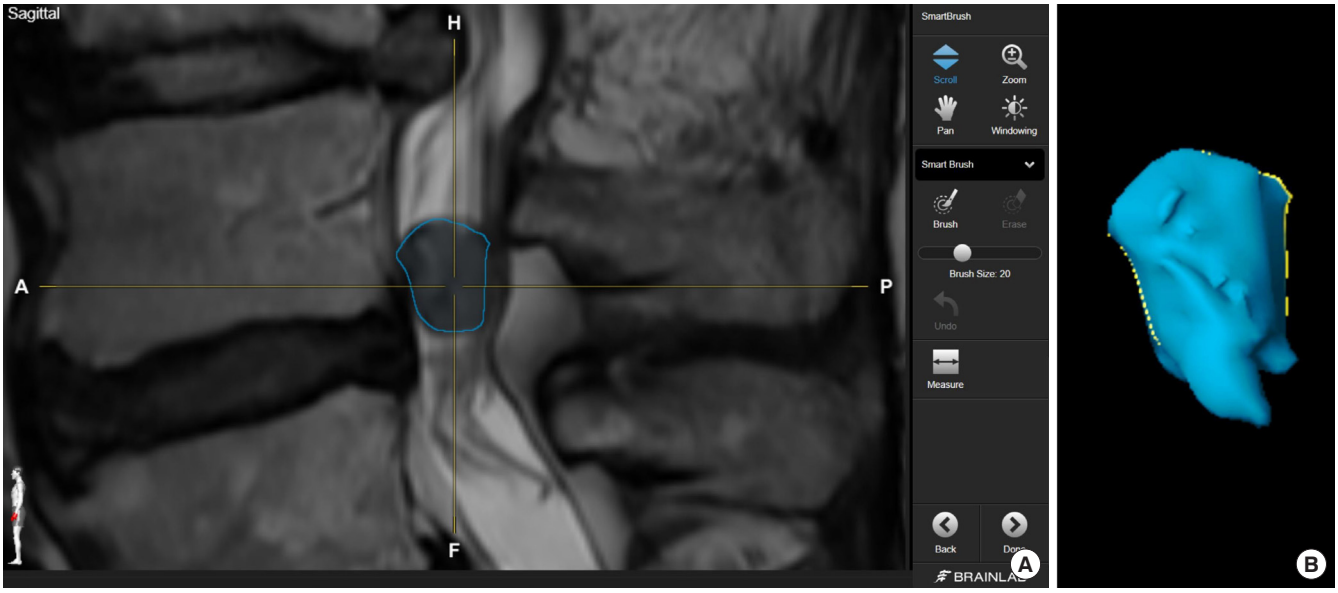

Fig. 1. (A) Highlighting of the neoplasm on a preoperative magnetic resonance imaging (MRI) using Brainlab elements software. (B) The "smartbrush" function of the software automatically renders the 2-dimensional highlighting on the MRI into a 3-dimensional shape.

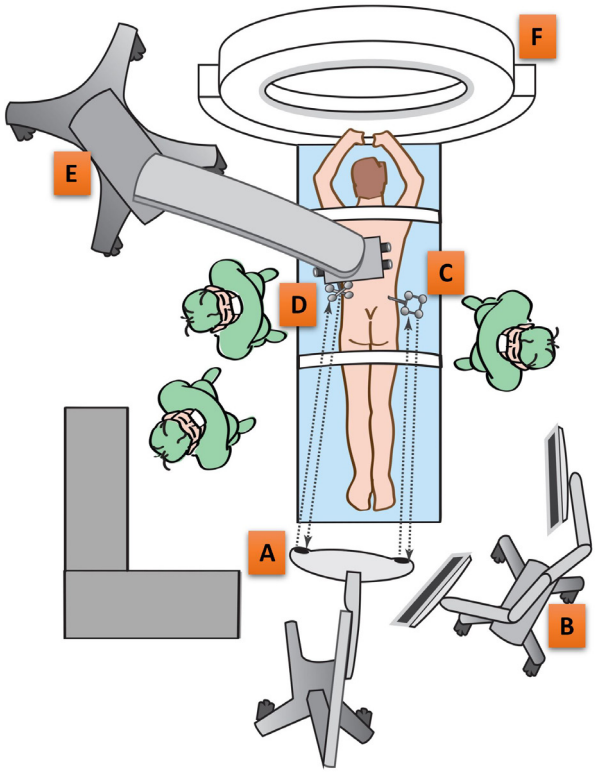

Fig. 2. Operating room setup for augmented reality navigation for a left sided approach. (A) Navigation camera. (B) Navigation screen. (C) Patient reference array. (D) Microscope reference array. (E) Microscope. (F) intraoperative computed tomography.

sition and the preoperative MRI in supine position, the image fusion included a correction of the different lordosis or kyphosis angles using elastic image fusion (Brainlab Curvature correction).[10] For this procedure, one vertebra in the MRI scan needs to be manually matched with the same vertebra on the CT scan, then the software corrects the curvature differences of the other levels. For maximal accuracy of the AR projection, we recommend manually matching the vertebra that is closest to the pathology to minimize deviation caused by the digital correction software (Fig. 3).

After each image fusion, the accuracy of fusion was verified and approved by a fellowship-trained orthopedic spine surgeon who was not involved in the surgical procedure. To avoid inaccuracy during the fusion process, the responsible person should have a basic understanding of the spinal anatomy. After validation of the digital image fusion, the highlighted tumor was visible on the navigation CT scan and could immediately be used for approach planning without any additional workflow steps (Figs. 4-8).

To integrate the surgical microscope view with the navigation system, calibration of the microscope to the AR software is necessary. For that purpose, a reference array is attached to the microscope and the microscope is connected to the navigation system using a dedicated data-cable for the transmission of the AR signal. For calibration of the microscope, the patient's reference array, which is attached on an anatomical structure close to the

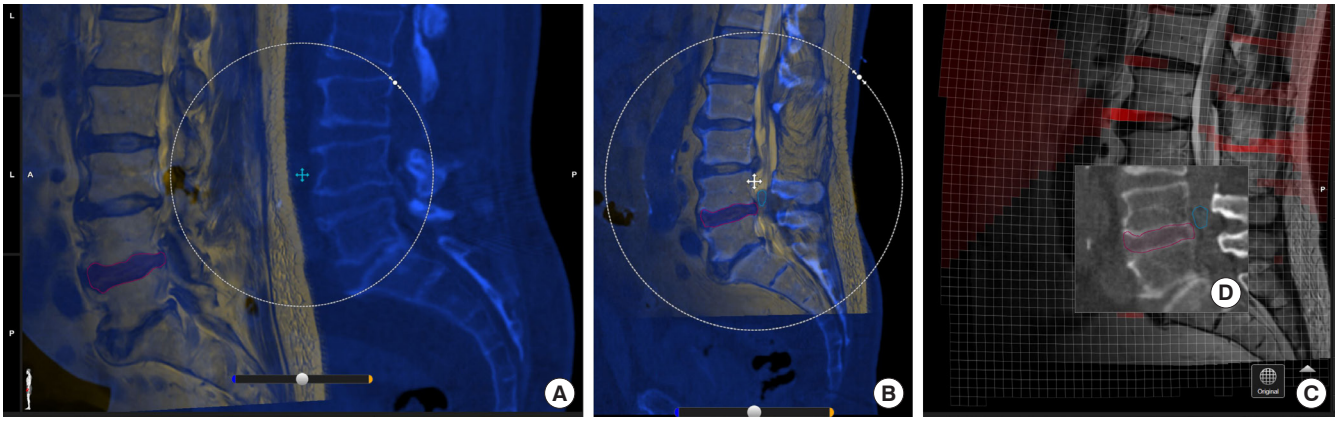

Fig. 3. (A) Elastic image fusion of the preoperative planning magnetic resonance imaging (MRI) scan (yellow) and the intraoperative navigation computed tomography (CT) scan (blue). (B) The scans are manually calibrated to be most accurate on the level closest to the surgical site. After elastic image fusion, the accuracy must be confirmed by superimposing the CT (small square [D]) onto the MRI. The red color shows the areas where the elastic image fusion software corrected the curvature of the spine. The intensity of the color is proportional the amount of correction (greater color intensity indicated greater curvature correction by the software).

Fig. 4. After confirmation of the accuracy of the image fusion, the preoperative highlighted neoplasm (blue) on the magnetic resonance imaging (A) is transferred to the intraoperative computed tomography scan (B).

pathology, must be viewed and focused through the surgical microscope's field of view. The patient's reference array is automatically detected by the navigation system in calibration mode when focusing the microscope on it and can be calibrated to the microscope (Fig. 9).

After calibration, the preoperatively highlighted structures were projected into the surgical microscope (Zeiss Pentero, Carl Zeiss Meditec, Jena, Germany) via the AR module. All procedures were recorded through the microscope. During surgery, the tumor location, and margins were projected into the surgeon's field of view via the microscope. The surgeon could turn the projection off if a clearer view of the surgical area was required (Figs. 10-16).

Surgery-specific data including the volume of the tumor, duration of surgery in minutes, and intraoperative blood loss were recorded. Also recorded was the time required for calibration of the AR. Additionally, when a tubular MIS approach was used, the time from tissue dilation until the tumor was reached was also recorded.

RESULTS

A total of 8 consecutive patients were included in our series (5 males) with a mean age of 56 ± 12 years. The mean BMI was

https://doi.org/10.14245/ns.2244222.111

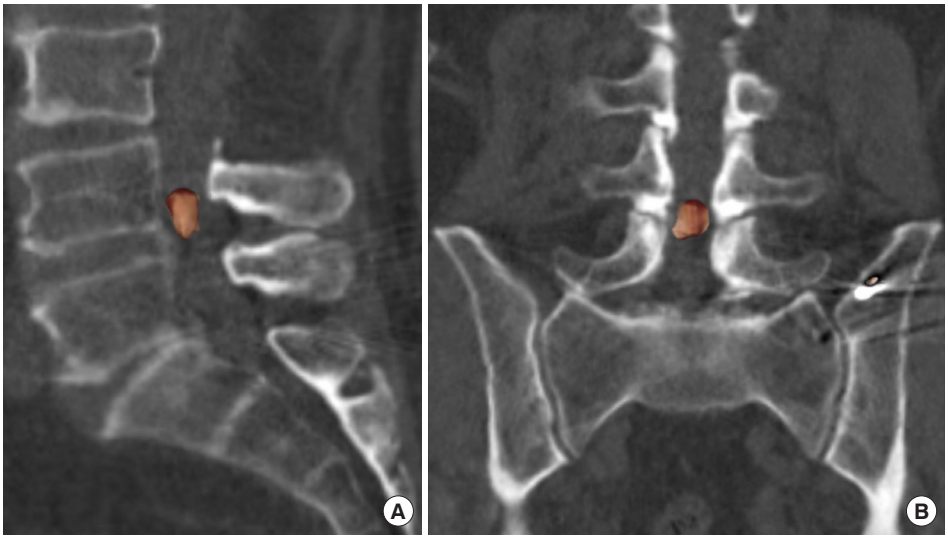

Fig. 5. The highlighted neoplasm can be displayed in 3-dimensional shape on the intraoperative computed tomography scan (sagittal view [A] and coronal view [B]).

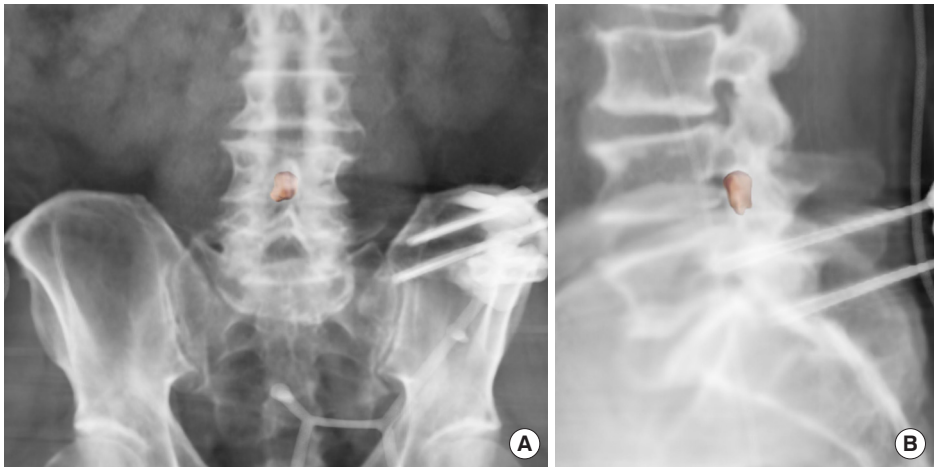

Fig. 6. Alternatively, the highlighted neoplasm can be displayed in 3-dimensional shape on reconstructed x-ray images from every angle to facilitate the orientation. A reconstruction of an anteroposterior view x-ray (A); A reconstruction of a lateral view x-ray (B).

28.7 ± 3.1 kg/m^2. The ASA PS classification was II in 7 patients and 1 patient had an ASA PS classification of III, respectively. The demographics of our study group are summarized in Table 1.

Four tumors were located at the lumbar spine (50%) and 4 (50%) in the thoracic spine. The average overall tumor volume was 1.4 ± 0.6 mL. Divided into MIS and open procedures the average volume of MIS resected tumors was 1.0 ± 0.5 mL and the average tumor volume of open cases was 1.5 ± 0.6 mL. According to histological evaluation of the intraoperative specimens, 5 of the cases were World Health Organization (WHO) grade I schwannoma, 1 WHO grade 1 meningioma, 1 WHO grade 1 paraganglioma, and 1 WHO grade 2 myxopapillary ependymoma. All tumors were located intradural and extramedullary.

A tubular MIS technique was used to resect 3 tumors (38%), while the other 5 tumors (62%) were resected using a traditional open approach. The skin incision in the MIS cases was around 3 cm and either 24-mm or 26-mm tubes were used. The overall average procedure time was 177 ± 58 minutes and the average overall blood loss was 186 ± 183 mL. Divided into open and MIS procedures the average operative time for MIS cases was 128 ± 8 minutes and for open cases 206 ± 55 minutes. The estimated intraoperative blood loss was 97 ± 77 mL in MIS procedures and 240 ± 206 in open procedures. The median overall hospital stay

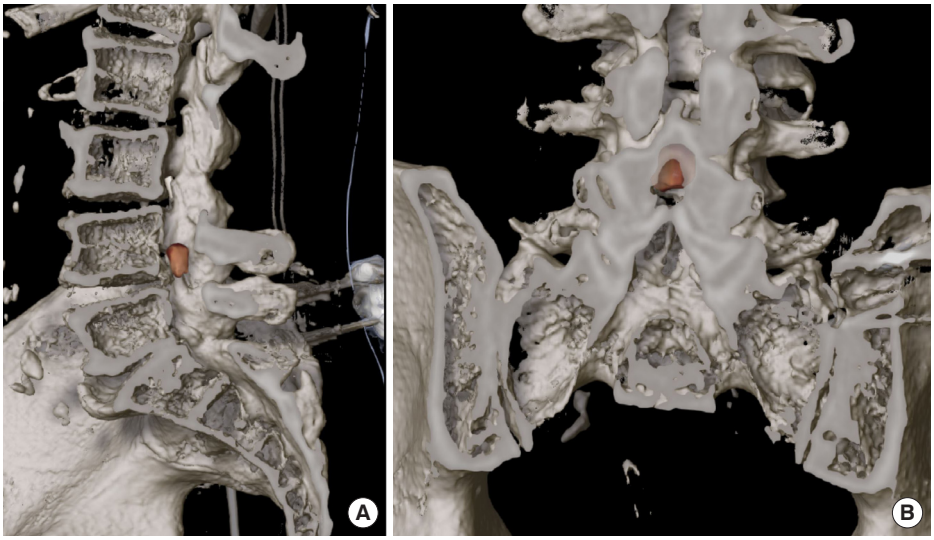

Fig. 7. A bony 3-dimensional (3D) reconstruction of the computed tomography (CT) scan allows to demonstrate the space conditions in relation to the tumor size in the spinal canal. Image (A) A lateral view of 3D reconstruction on CT scan. (B) A posterior view of 3D reconstruction on CT scan. The digital cut allows to view the neoplasm and estimate the space conditions.

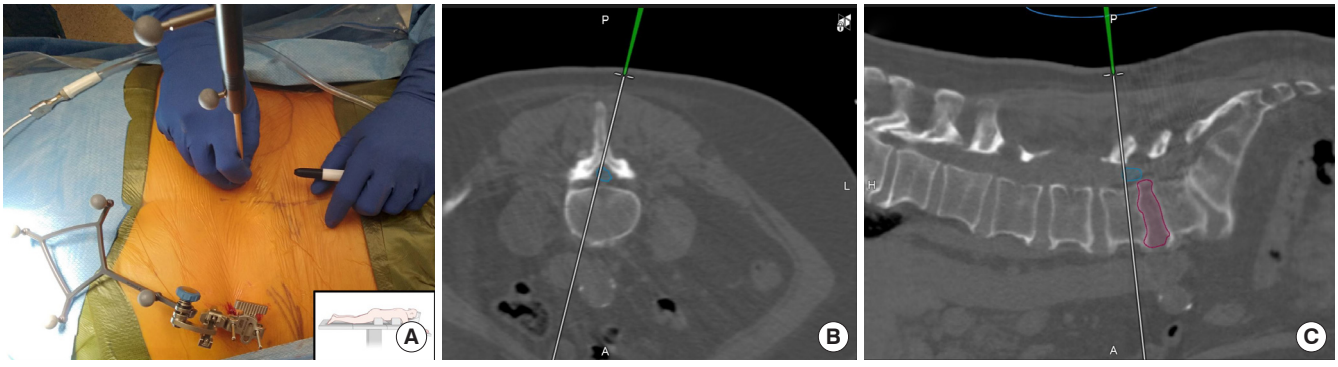

Fig. 8. (A) Planning of the surgical approach using a navigated pointer. The navigation shows the trajectory of the pointer on the coronal (B) and sagittal (C) view of the intraoperative computed tomography scan. Even during the approach planning the shape of the neoplasm is visible (blue) and the closest disc space (red).

was 4 ± 4.6 days. A detailed list of surgical times and treated pathologies is shown in Table 2.

Preoperative weakness was reported in 6 cases (67%) and numbness was reported in 3 cases (33%). Postoperatively, the muscle weakness was improved in 5 cases and only 1 patient showed persistent weakness. Numbness improved in 2 cases and only 1 patient showed persistent numbness. Additionally, 1 patient reported new numbness after surgery.

In all cases, the AR support was available at the time the microscope was used and no additional delay was caused. The elastic image fusion took place in the background to the actual surgery and the navigation system was fully operational in parallel, therefore this also did not lead to any delay in the actual surgical procedure. The only additional step that had to be integrated into the surgical workflow was the calibration of the microscope. This step required an average of 1.6 ± 1.2 minutes to calibrate the microscope to the navigation system.

The precision of the AR was sufficiently accurate in all cases and corresponded to the actual limits of the tumor. The accuracy of navigation was regularly checked during surgery using exposed anatomic landmarks such as the spinous processes. Subjective accuracy on the part of the surgeon was reported to be < 2 mm. Neither correction of the approach trajectory or ultrasonic assistance was required in any case nor a conversion to an open procedure in any MIS case. No intraoperative complications were observed. The intraoperative pathology result showed be-

 https://doi.org/10.14245/ns.2244222.111

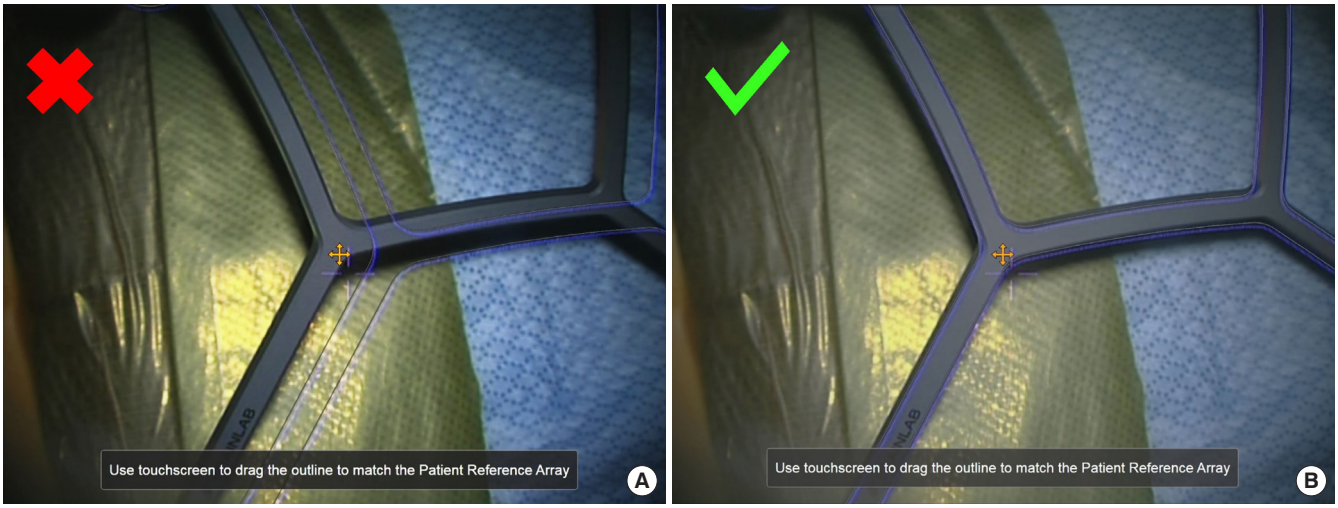

Fig. 9. Intraoperative calibration of microscope to patient reference array. (A) Microscope view pre calibration. The virtual frame does not match the reference array. (B) Microscope view after calibration. The virtual frame matches the reference array.

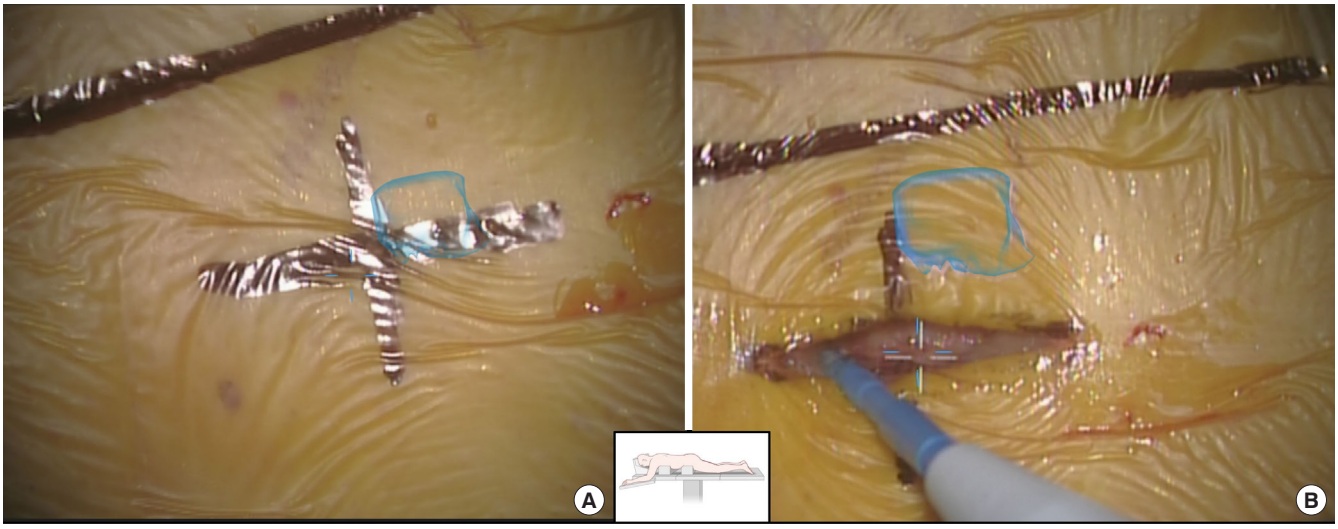

Fig. 10. (A) Surgical site before skin incision. (B) Surgical site after dissection of the skin. The projection stays in place. After calibration of the microscope, the highlighted neoplasm is projected into the surgeon's field of view (blue shape). The shape of the augmented reality (AR) projection matches with the navigated planning of the approach (cross on image A). Soft tissue preparation for the tubular approach after skin incision with AR visible (blue shape).

nign tumors in all cases. Depending on location, either a total resection of the tumor was performed or if the tumor affected a motor nerve root, maximally-safe debulking was performed to avoid injury of the motor nerve. The regular follow-up recommendation for these patients is an MRI scan after 3 months. There were no revision surgeries in the 2-week short-term follow-up.

DISCUSSION

AR technology offers a promising advancement for tumor resection utilizing the tubular MIS technique. Until recently, resection of BIET was limited via tubular minimally invasive approaches due to the lack of ultrasound probes small enough to be inserted through a tubular retractor.[5,6] Today, ultrasound probes are available that are small enough to be used through tubular retractors.[6] However, handling remains challenging, requires a high level of experience and interrupts the surgical workflow. In addition, the ultrasound probe can first be utilized after the dura exposure and is not available during the approach planning or to determine the bone removal to approach the tumor. Orientation up to that point is accomplished by x-ray or navi-

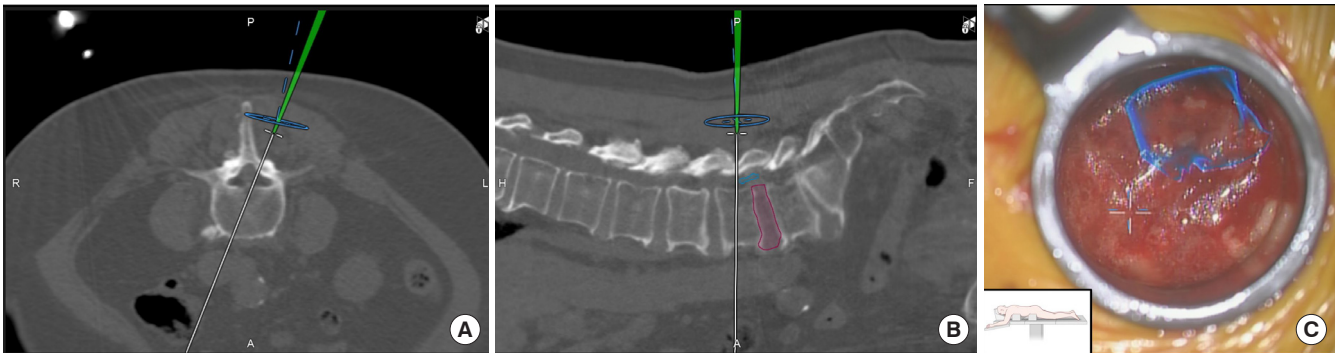

Fig. 11. Confirmation of the approach trajectory after placement of the tubular retractor using 3-dimensional navigation in coronal (A) and sagittal view (B). Panel C shows the intraoperative view through the microscope after placement of the tubular retractor. The size, shape, and location of the neoplasm (blue shape) is visible during the soft tissue dissection.

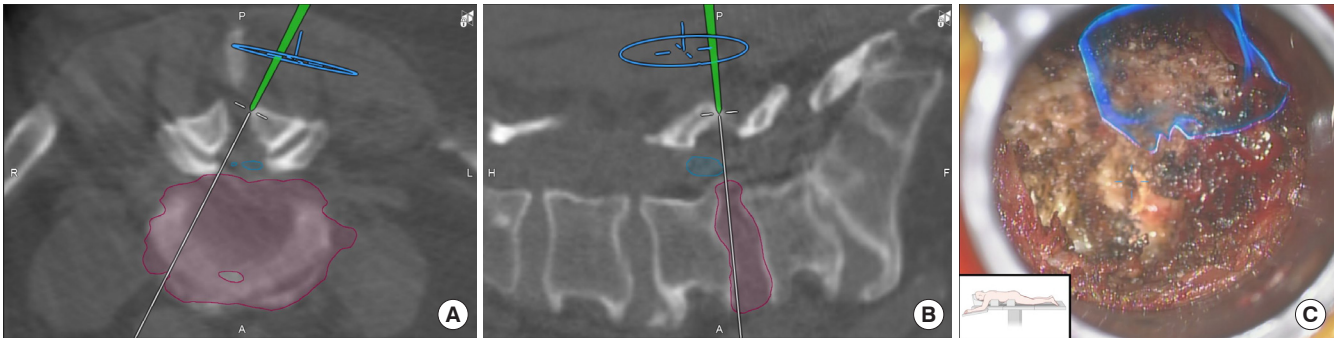

Fig. 12. Confirmation of the anatomy after soft tissue dissection but before laminectomy in coronal (A) and sagittal (B) view. Panel C shows the microscopes view on the exposed left sided lamina of L4. The neoplasm is highlighted blue.

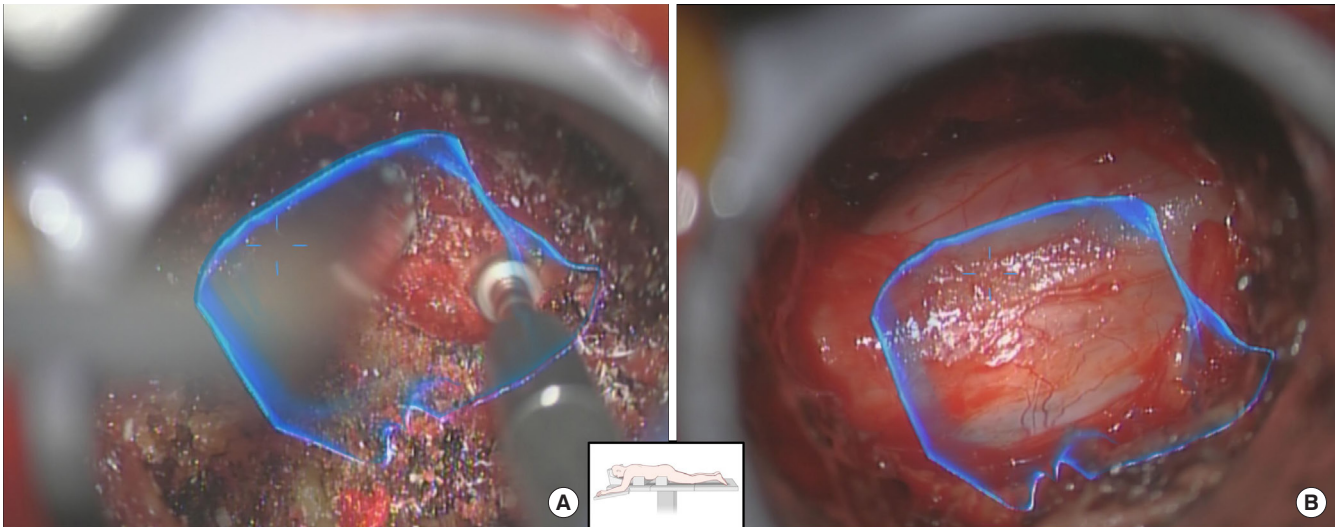

Fig. 13. Projection of the tumor site during removal of the bony structures (A) and when the dura is exposed (B).

gation to the location where the tumor is expected to be located.[9] By using AR, it is possible to see the actual position and the size of the tumor even during the approach planning as shown in Fig. 10. This allows precise planning of the skin incision and accurate placement of the tubular retractor, which minimizes soft tissue damage. As a result, a precise laminectomy can be performed to provide enough space to approach the tumor safely. This limited resection of bone further reduces iatrogenic in-

https://doi.org/10.14245/ns.2244222.111

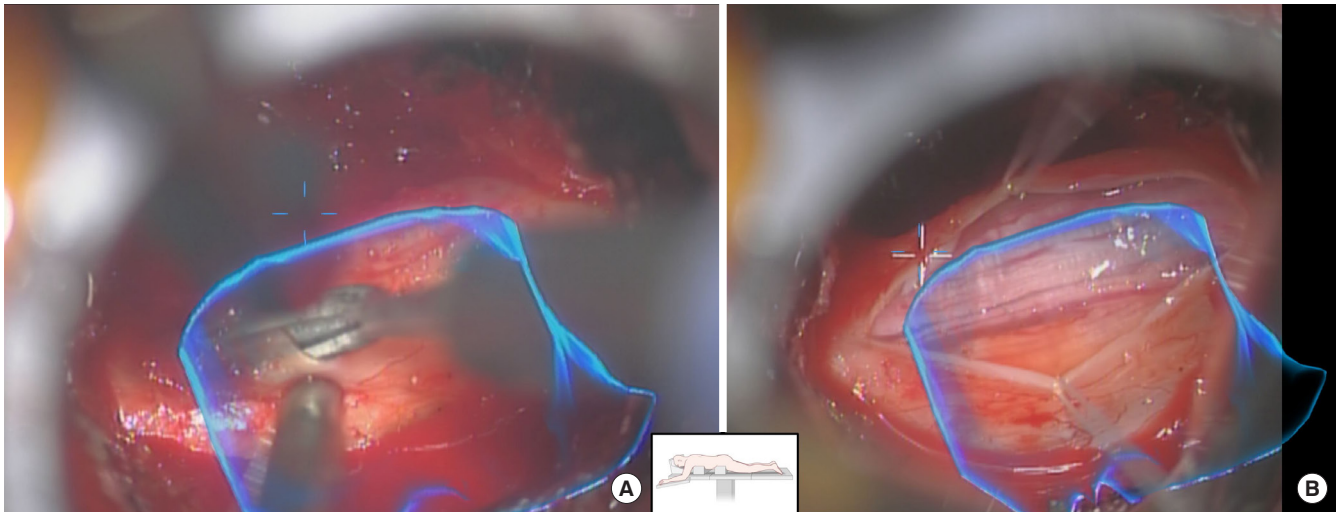

Fig. 14. (A) The projection allows an exact incision of the dura. (B) After the incision, the dura is held open using holding sutures on both sides of the tubular retractor.

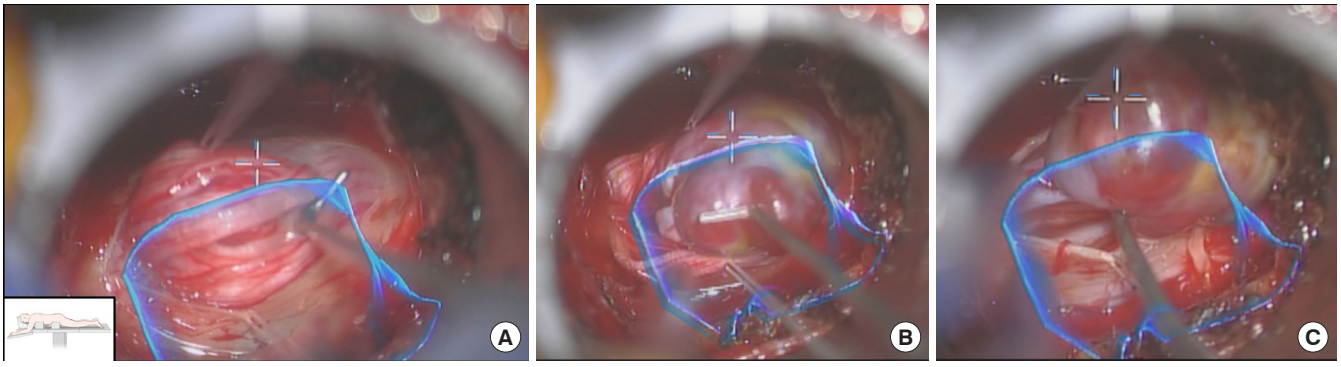

Fig. 15. (A, B) Exposure and resection of the neoplasm. After the incision of the dura, the neoplasm is found at the location of the augmented reality projection. Panel C shows the resection of the neoplasm under neuromonitoring.

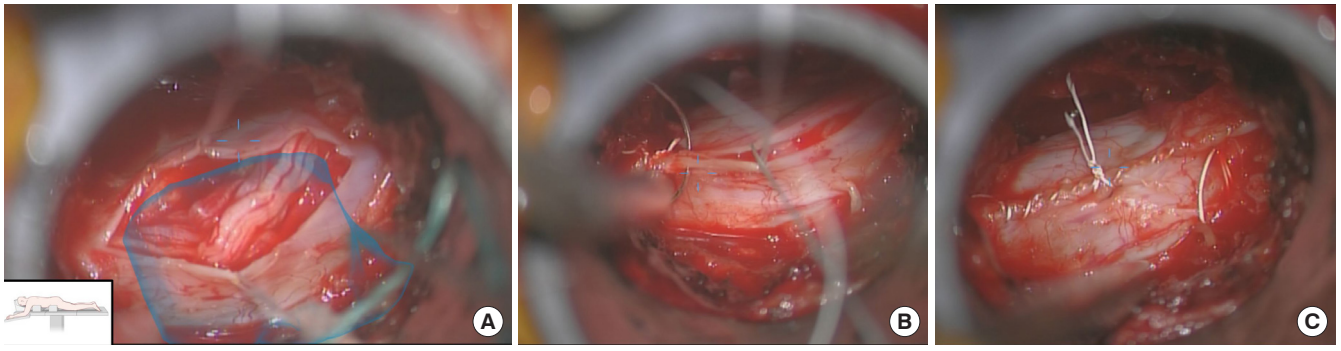

Fig. 16. Closure of the dura after resection of the neoplasm. Panel A shows the conditions at the surgical site after the removal of the neoplasm and the size of the neoplasm (blue shape) in relation to the dura incision. (B) After resection, the augmented reality support is turned off and the dura is closed by suture via the tubular approach. Panel C shows the final result after closure of the dura.

stability of the spinal segment and avoids long-term postoperative complications.

The integration of AR into the regular surgical procedure was efficient in our case series. The image fusion between the

preoperative MRI with AR planning and the intraoperative CT can be performed in parallel with the other surgical steps and did not interrupt the workflow, nor did it not cause any delay of the surgical procedure in our evaluation. The only additional step that needed to be performed was the calibration of the microscope to the navigation system to accurately perform the AR projection. In our case series, the calibration of the microscope took 1.6 ± 1.2 minutes, which is an insignificant delay.

The accuracy of projecting the AR into the microscope corresponded exactly to the position of the tumor in all cases. The correct visualization of the cranial and caudal tumor borders is essential here since the surgical approach is chosen according to these 2 borders and the laminectomy is performed in reference to the BIET's location. Extension of the approach was not necessary in any of the cases. Furthermore, in 1 case of tumor with an irregular shape and extension of the tumor into the neuroforamen, AR-guidance was key to achieving gross total resection.

Table 1. Demographics of the study population

Patient No.	Sex	Age (yr)	BMI (kg/m^2)	ASA PS classification	Level of pathology	Preop. weakness	Preop. numbness
1	F	45	29.1	II	L5/S1	Yes	No
2	M	50	32.0	III	T1/2	Yes	Yes
3	F	59	24.9	II	T10/11	Yes	No
4	M	82	29.0	II	L4/5	No	No
5	M	60	34.2	II	L2	Yes	Yes
6	F	53	26.9	II	L5/S1	No	Yes
7	M	42	28.6	II	T1	Yes	No
8	M	53	24.6	II	T6/7	Yes	No

BMI, Body mass index; ASA PS, American Society of Anesthesiologists physical status; T, thoracic; L, lumbar; preop., preoperative.

This study, to our knowledge, is the first study on AR-assisted resection of BIET involving the lumbar spine. In contrary to the cervical and thoracic spine, most lumbar BIET do not cause compression of the spinal cord but rather the nerve roots of the cauda equina.[11] This bundle of nerves provides flexibility which the surgeon can use to their advantage in terms of retraction and manipulation. In some situations, the tumor suspension in cerebrospinal fluid can cause variation in positioning concomitant with the respiratory cycle. This creates an obstacle for accurate AR projection, since the projection shows only the preoperatively planned position and does not dynamically adapt to changes in tumor position during surgery. This theoretical limitation of accuracy was not observed in our study. In our case series, there was no relevant cranial or caudal dislocation before finding the tumor. Likewise, opening the dura did not result in any relevant inaccuracy of the AR projection. The opening of the dura was always performed at the level of the AR projection and corresponded to the actual position of the tumor in all cases. This observation is consistent with the previously described high accuracy of the AR projection in other studies.[8,12] Nevertheless, during the actual tumor resection particularly for schwannomas, attention should be paid to begin resection and disconnection from the cranial rather than the caudal end to avoid subsequent cranial retraction of the tumor which may require extension of the laminectomy.

After resection of the tumor, AR was found helpful in the lumbar spine to inspect the resection site for any residual tissue before closing. Since it is often not possible to remove the tumor *en bloc*, continued projection of the original tumor margins after resection helped to thoroughly explore the intradural space in the highlighted area and search for possible tumor fragments to ensure that all tumor components were completely re-

Table 2. Final pathological results, tumor volume, procedure time, estimated blood loos, hospital stay, and surgical approach

Patient No.	Pathology	Tumor volume (mL)	Procedure time (min)	Estimated blood loss (mL)	Hospital stay (day)	Surgical approach
1	Schwannoma WHO grade I	1.59	120	15	2	Tubular MIS
2	Schwannoma WHO grade I	2.12	263	600	7	Open
3	Meningioma WHO grade I	0.55	165	0	17	Open
4	Paraganglioma WHO grade I	1.11	140	75	6	Tubular MIS
5	Myxopapillary ependymoma WHO grade 2	1.69	146	300	3	Open
6	Schwannoma WHO grade I	0.43	125	200	2	Tubular MIS
7	Schwannoma WHO grade I	1.35	282	200	5	Open
8	Schwannoma WHO grade I	1.97	174	100	3	Open

WHO, World Health Organization; MIS, minimally invasive surgical.

https://doi.org/10.14245/ns.2244222.111

moved. This is especially challenging in the lumbar spine where tumor fragments can easily be overlooked due to the many mobile nerves of the cauda equina.

There are limitations of our study. First, the low number of patients in this series is too small to draw general conclusions. Whether the positive first impression of the use of AR in resection of BIETs can be maintained in a larger and more diverse case series needs to be investigated. Second, the software used required manual marking of the tumor on the preoperative MRI, which increases the preoperative planning time. In all cases, preoperative marking required only a few minutes and did not add a significant effort to the procedure workflow. In the future, advancement of the software may allow automatized identification of the pathology and reduce the preoperative planning time. Additionally, highlighting the tumor manually may present error, since irregular tumor borders on MRI or incorrect margins due to surrounding nerves which appear like the tumor may cause the person doing the marking to incorrectly outline the tumor.

Another limitation of the technique is that intraoperative navigational CT is required, which exposes the patient to additional radiation. However, the use of total intraoperative navigation is at present a well-established and frequently used technique.[9,13] For surgeons who are already using navigation as part of their surgical workflow, the use of AR does not require any additional radiation, since the software uses the navigation data set. AR thus represents a useful extension to existing navigation capabilities. In addition, intraoperative navigational CTs typically use low-dose protocols, which keep patient radiation exposure low. Operating room staff can even leave the operating room during the CT and completely avoid radiation exposure.[9,14] Overall, the use of AR in the detection of spinal tumors is a safe and effective alternative or adjunct to existing intraoperative orientation methods such as ultrasound, particularly for minimally invasive approaches.

CONCLUSION

The use of AR in the resection of intradural extramedullary tumors allows reproducible accurate visualization of the tumor level and position within the dura. AR-guidance can be integrated into the workflow of surgery without significant alterations to the standard routines and does not cause significant prolongation of surgery. Further studies are required to further elucidate the advantages of AR over ultrasonic guidance especially for minimally invasive surgical approaches in combination with 3D navigation.

NOTES

Conflict of Interest: Roger Härtl is a consultant for Ulrich, Brainlab, DePuy-Synthes and has royalties from Zimmer. Fabian Sommer received speaker fees from Baxter.

Funding/Support: This study received no specific grant from any funding agency in the public, commercial, or not-for-profit sectors.

Author Contribution: Conceptualization: FS, IH, SK, RH; Data curation: FS; Formal analysis: FS, RH; Funding acquisition: FS, RH; Methodology: FS, IH, SK, JG, LM, FW, FS, RH; Project administration: FS, RH; Visualization: FS, IH, SK, JG, LM, RNR, FW, FSc, PG, RH; Writing - original draft: FS; Writing - review & editing: IH, SK, JG, LM, RNR, FW, FS, PG, RH

ORCID

Fabian Sommer: 0000-0002-6284-7042
Jacob Goldberg: 0000-0003-0827-9387
Pravesh Shankar Gadjradj : 0000-0001-9672-4238
Roger Härtl: 0000-0003-2442-8944

REFERENCES

1. Duong LM, McCarthy BJ, McLendon RE, et al. Descriptive epidemiology of malignant and nonmalignant primary spinal cord, spinal meninges, and cauda equina tumors, United States, 2004-2007. Cancer 2012;118:4220-7.
2. Ottenhausen M, Ntoulias G, Bodhinayake I, et al. Intradural spinal tumors in adults—update on management and outcome. Neurosurg Rev 2019;42:371-88.
3. Arnautovic K, Arnautovic A. Extramedullary intradural spinal tumors: a review of modern diagnostic and treatment options and a report of a series. Bosn J basic Med Sci 2009; 9(Suppl 1):40-5.
4. Prada F, Vetrano IG, Filippini A, et al. Intraoperative ultrasound in spinal tumor surgery. J Ultrasound 2014;17:195-202.
5. Hernandez RN, Kirnaz S, Schmidt F, et al. Minimally invasive surgery for intradural tumors. In: Hanft S, McCormick PC, editors. Tumors of the spinal canal. Cham: Springer International Publishing; 2021:181-200.
6. Krüger MT, Steiert C, Gläsker S, et al. Minimally invasive resection of spinal hemangioblastoma: feasibility and clinical results in a series of 18 patients. J Neurosurg Spine 2019

Aug 9:1-10. https://doi.org/10.3171/2019.5.SPINE1975. [Epub].
7. Sommer F, Goldberg JL, McGrath L Jr, et al. Image guidance in spinal surgery: a critical appraisal and future directions. Int J Spine Surg 2021;15(s2):S74-86.
8. Carl B, Bopp M, Saß B, et al. Augmented reality in intradural spinal tumor surgery. Acta Neurochir (Wien) 2019;161: 2181-93.
9. Navarro-Ramirez R, Lang G, Lian X, et al. Total navigation in spine surgery; a concise guide to eliminate fluoroscopy using a portable intraoperative computed tomography 3-dimensional navigation system. World Neurosurg 2017;100: 325-35.
10. Schmidt FA, Mullally M, Lohmann M, et al. Elastic image fusion software to Coregister preoperatively planned pedicle screws with intraoperative computed tomography data for image-guided spinal surgery. Int J Spine Surg 2021;15:295-301.
11. Diaz E, Morales H. Spinal cord anatomy and clinical syndromes. Semin Ultrasound CT MR 2016;37:360-71.
12. Zhao J, Liu Y, Fan M, et al. Comparison of the clinical accuracy between point-to-point registration and auto-registration using an active infrared navigation system. Spine (Phila Pa 1976) 2018;43:E1329-33.
13. Härtl R, Lam KS, Wang J, et al. Worldwide survey on the use of navigation in spine surgery. World Neurosurg 2013; 79:162-72.
14. Sarwahi V, Payares M, Wendolowski S, et al. Low-dose radiation 3D intraoperative imaging. Spine (Phila Pa 1976) 2017; 42:E1311-7.

 https://doi.org/10.14245/ns.2244222.111